Low cycle fatigue behaviour and life prediction of Q345B steel and its welded joint

You, X. , Liu, Y. J. , Khan, M. K. and Wang, Q. Y.

Low cycle fatigue behavior and life prediction of Q345B steel and its welded joint

X. You[1], Y. J. Liu[2], M. K. Khan[1,2], Q. Y. Wang*[1,3]

1: Key Laboratory of Energy Engineering Safety and Disaster Mechanics, Ministry of Education, College of Architecture and Environment, Sichuan University, Chengdu 610065, China

2: Department of Mechanical Engineering, DHA Suffa University, DHA 75500, Karachi, Pakistan

3: School of Urban and Rural Construction, Chengdu University, Chengdu 610106, China

*Corresponding author: wangqy@scu.edu.cn

Abstract: Low cycle fatigue (LCF) behavior of Q345B steel and its smooth welded joint were experimentally investigated in fully reversed strain-control at constant strain rate of 0.005 s^{-1}. The cyclic stress response characteristics, strain-life and strain-energy relationships were obtained and analyzed in the strain regime 0.3%-0.7%. It was found that Q345B showed significant cyclic hardening and softening above and below the 40% strain amplitudes, respectively. The welded joints showed cyclic hardening in the entire strain regime due to the mechanical inhomogeneity. The low cycle transition life, fatigue strength and fatigue life of welded joint were found significantly lower with increase in the cyclic hardening. The experimental data was used to extract the Coffin-Manson parameters and the strain-life relationship. In addition, the expressions of plastic strain energy and fatigue life were also obtained using the energy prediction method.

Key words: Q345B, smooth welded joint, low cycle fatigue, fatigue life, life prediction

Introduction

Q345B is a low alloy steel with excellent comprehensive mechanical properties. It provides high strength, fine plasticity, ductility and solderability. It is widely used in automobiles, ships, pressure vessels, especially civil engineering structures such as bridge, construction, and offshore structures etc. . In such engineering structures, welding is extensively used as a joining technique.

Fatigue fracture under low cycle fatigue (LCF) has always been considered as one of the main failure type of structures [1]. Most civil engineering components made of Q345B steel are often subjected to cyclic loading in service. For examples, highway bridges often subject to dynamic load including cyclic and/or random fluctuations; pressure vessels always endure cyclic loading caused by start-stop operations or fluctuations of working pressure. In the welded structures, welded joints are always considered as the weakest part and prone to failure due to fatigue [2]. Therefore, to develop a better understanding of the material/component selection or replacement, fatigue behaviors of Q345B steel and its welded joint under cyclic loading has been carried out.

In the past decades, the low cycle fatigue behaviors such as cyclic energy absorption rate, cyclic response characteristic, life prediction, fracture mechanism and so on, have been studied in many structural steels including carbon steels [3-6], and stainless steels [6-8]. It has been observed that the fatigue failure in LCF regime is caused by plastic strain. The plastic strain-life data can be evaluated by the Coffin-Manson law [9,10]. The analysis methods of fatigue on welded joint were well reviewed by Fricke [11] previously and many studies on fatigue behavior of welded joint were summarized recently [12], which concerned the effects of discontinuity, geometry, stress ratio and residual stress on the fatigue behaviors of welded structures [13]. However, to the authors' knowledge, there is no report on the fatigue behaviors of Q345B

steel and its welded joint.

In this paper, LCF tests on Q345B steel and its welded joint were conducted and the results were used to validate the Ramberg-Osgood relationship and Coffin-Manson relationship. In addition, fatigue life predictions on both Q345B base metal and welded joint were also carried out.

1 Experimental procedures

The material used in this study was a commercial Q345B steel. The nominal chemical compositions of the materials are C-0.16, Si-0.35, Mn-1.34,S-0.11, P-0.22(wt%) . The mechanical properties are as follows: E=201 GPa, σ_s=395 MPa and σ_b=550 MPa.

For the welded joints, two base metal plates were initially welded together using the tungsten inert gas (TIG) arc welding method and then the welded specimens were prepared from the plates. The base metal and weld specimens were designed according to the Chinese standard of GB/T 15248-1994 [14] which had a diameter of 8 mm in the test segment and a gauge length of 20 mm. The specimen dimensions were kept to avoid buckling phenomena under the highest compressive forces anticipated in the test program. Before test, all the specimens were first mechanically polished using sandpaper from grade 600 to grade 2000 in sequence and then further polished with diamond suspensions with minimum grain size of 1μm.

A servo-hydraulic testing machine (EHF-EM200k2-040, made by Shimadzu was used for testing in ambient air at room temperature. The tests were carried out under uniaxial tension-compression loading with a strain ratio of - 1, and the uniaxial extensometer with a gauge length of 12.5 mm was used to measure the strain. The symmetric strain-controlled LCF tests were carried out for the strain amplitudes of 0.3, 0.4, 0.5, 0.6, 0.7% with a constant strain ratio of 0.005/s, and triangular waveform was used for all the fatigue tests. For each strain amplitude, three specimens were tested in order to obtain effective data.

2 Results and discussion

2.1 Cyclic stress-strain curve

From the obtained result of the variation of stress amplitude at the ratio of cyclic number (N) to fatigue life (N_f) during testing process, it is found that the material exhibits cyclic hardening or softening at the initial loading cycles, and then the response curve stabilizes until the fatigue crack initiates.

When a family of stabilized hysteresis loops at different strain amplitudes is plotted on the same graph, a cyclic stress-strain curve can be obtained by tracing the locus of the tips of the loops. The response at N/N_f=0.5 can be used to obtain cyclic stress-strain curves, and the cyclic stress-strain relationship may be represented by a form of Ramberg-Osgood relationship as follows []

$$\frac{\Delta\varepsilon}{2}=\frac{\Delta\varepsilon_e}{2}+\frac{\Delta\varepsilon_p}{2}=\frac{\Delta\sigma}{2E}+\left(\frac{\Delta\sigma}{2K'}\right)^{1/n'} \quad (1)$$

where Δσ is the stress range, [MPa]; Δε is the total strain range; $\Delta\varepsilon_e$ is the elastic strain amplitude; $\Delta\varepsilon_p$ is the plastic strain amplitude; E is the Young's modulus, [MPa]; K' is the cyclic strength coefficient, [MPa]; n' is the cyclic strain hardening exponent.

The characteristics of cyclic hardening or softening are related to cyclic stress-strain curves, which can be evaluated with reference to the monotonic curve [15]. Q345B shows significant cyclic hardening or softening respectively when the strain amplitudes are larger or lower than 0.4%, while welded joint shows obvious cyclic hardening in the whole strain regime of 0.3~0.7%.

Comment [U1]: Is it correct?. The abstract says 40%

The material coefficients K' and n' can be obtained through a power law regression fitting of the stress amplitude Δσ versus plastic strain amplitude data $\Delta\varepsilon_p$. The average values of elastic strain, stress amplitude and fatigue life are listed as Tab.1, and K' and n' can be derived from the results as K'=563.9, n'=0.1611 (for base metal), and K'=642.05, n'=0.1638 (for welded joint), which will be used in the low cycle fatigue analysis and evaluation of Q345B base metal and welded joint. The fitting curves of cyclic stress-strain data

for Q345B base metal and welded joint are illustrated as solid line and dash line respectively in Fig.1. It can be seen that the stabilized stress amplitudes of base metal and welded joint both increase with the increase of strain amplitude. Meanwhile, the stress value of the base metal was found higher than those of welded joint at the same loading strain amplitude.

Table.1 Average results of the fatigue tests

Total stain (%)		Elastic strain (%)	Plastic strain (%)	Stress (MPa)	Fatigue life
0.3	Base metal	0.1681	0.1319	353	6200
	Welded joint	0.1814	0.1186	381	3227
0.4	Base metal	0.1733	0.2267	364	4105
	Welded joint	0.1986	0.2014	417	2221
0.5	Base metal	0.1910	0.3090	401	2360
	Welded joint	0.2023	0.2977	425	1338
0.6	Base metal	0.1986	0.4014	417	1228
	Welded joint	0.2280	0.3720	479	834
0.7	Base metal	0.2052	0.4948	431	678
	Welded joint	0.2245	0.4755	471	575

2.2 Strain-life curve

The material parameters of the Coffin-Manson relationship can be calibrated by resolving the total strain into elastic and plastic components. Although the total strain amplitude was kept constant during the test, the amplitudes of elastic strain and plastic strain components would change due to cyclic hardening or softening. The elastic stain amplitude can be calculated from the stabilized stress amplitude at the half fatigue life according to the following equation:

$$\frac{\Delta\varepsilon_e}{2}=\frac{\Delta\sigma}{2E} \tag{2}$$

where the symbols have the same definitions as those in Eq.(1). Then, the plastic strain amplitude $\Delta\varepsilon_p$ is the difference of total strain amplitude $\Delta\varepsilon$ and elastic strain amplitude $\Delta\varepsilon_e$. Strain-based fatigue curves are usually used to describe low cycle fatigue of metals [16].The average results of each component at different strain amplitudes are used to determine the strain-life relationship.

The Coffin-Manson relationship [17, 18] can be expressed as follows:

$$\frac{\Delta\varepsilon}{2}=\frac{\Delta\varepsilon_e}{2}+\frac{\Delta\varepsilon_p}{2} \tag{3}$$

$$\frac{\Delta\varepsilon_e}{2}=\frac{\sigma_f^{'}}{E}(2N_f)^b \tag{4}$$

$$\frac{\Delta\varepsilon_p}{2}=\varepsilon_f^{'}(2N_f)^c \tag{5}$$

where $\Delta\varepsilon$ denotes total strain range, $\Delta\varepsilon_e$ denotes elastic strain amplitude, $\Delta\varepsilon_p$ denotes plastic strain amplitude, σ_f' denotes fatigue strength coefficient [MPa], b denotes fatigue strength exponent, $\varepsilon_f^{'}$ denotes fatigue ductility coefficient, c denotes fatigue ductility exponent, and N_f denotes number of

reversals to failure. Fitting the experimental data in Tab.1, the values of σ_f', b, ε_f' and c in the Coffin-Manson equation can be obtained as follows:

σ_f' =441, b =-0.094, ε_f' =0.1537, c =-0.559, for base metal;

σ_f' =588, b =-0.128, ε_f' =0.5445, c =-0.762, for welded joint.

The fitting curves are illustrated as Fig.6. It can be seen that the curves of base metal and weld joints agreed well with the experimental fatigue data. Thus, the obtained parameters can be used for low cycle fatigue analysis and life prediction of base metal and welded joint.

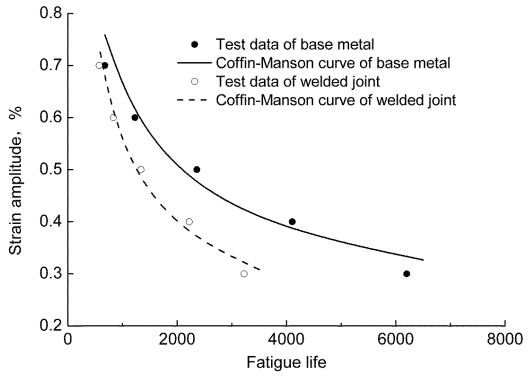

Fig.6 Strain-life curve

It was found that the low cycle fatigue strength and fatigue life of the welded joint are significantly lower than those of base metal. The fatigue life of the welded joint decreased exponentially with the strain amplitude. At 0.7% strain amplitude, the fatigue life of the welded joint was 85% of that of base metal, while it was only about 52% at the strain amplitude of 0.3%. Assuming that the fatigue strength can be evaluated by the strain amplitude, the fatigue strength of the weld joints was significantly lower than that of base metal at the same number of cycles. For example, at the fatigue life of N_f=2000 cycles, fatigue strength of the welded joint decreases by 21% relative to that of the base metal.

When the relationship curves of elastic strain amplitude ε_e and plastic strain amplitude εp versus fatigue life N_f are plotted on a graph, the intersection of such two curves can be defined as the transition point, and the corresponding life fatigue is the transition life N_t .The transition life N_t is an important parameter to evaluate fatigue property of material in the low cycle fatigue regime. When the number of cycles N<Nt, the fatigue behavior is dominated by the plastic strain amplitude; otherwise elastic strain amplitude plays a primary role. The εe-Nf and εp-N_f curves for the base metal and welded joint are shown in Fig.7. It can be seen that the εe-Nf curves for the base metal and welded joint are almost the same, whereas the εp-Nf curve of the welded joint is obviously lower than that of the base metal, which means the plasticity of the welded joint is significantly decreased. According to the test data, the transition life for the base metal and welded joint is determined as Nt=5112 and Nt=2038 respectively, namely, the transition life of the welded joint is reduced by 60% relative to the base metal.

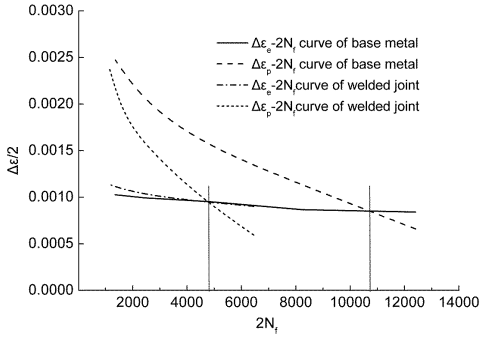

Fig.7 Curves of elastic strain and plastic strain versus life

Earlier studies have shown that [19], the initiation and propagation of fatigue cracks from welded joints is different from that in homogeneous base materials due to the high level of residual stresses, complex microstructure, strength mismatching, complex loading or internal defects found in welds. For the smooth welded joint, mechanical inhomogeneity (complex microstructure, strength mismatching or internal defects) can be the main reason that leads to the decrease of the low cycle fatigue strength, since the stress concentration effect caused by the geometric discontinuity of welded toes has been greatly mitigated. At high strain amplitudes, plastic deformation occurs at fusion and heat affected zones, and the plasticity and ductility at these zones are weak, which enhances cyclic hardening of the materials at these zones. From the SEM investigation of the fracture surfaces, welded defects (inclusions or gas pores) at these zones which introduced in the welding process were found to be preferable areas for fatigue crack initiation, as shown in Fig.8.

2.3 Prediction of crack initiation life

According to the characteristics of the cyclic stress-strain curves shown in Fig.4, the point from which the stress amplitude continually descends is usually defined as the demarcation point of fatigue crack initiation and growth [20].

Fig. 9 shows the obtained fatigue crack initiation life Ni at different strain amplitudes. For the base metal, the fatigue crack initiation time occupies more than 50% of the total life, and this proportion even reaches 95% at high strain amplitudes. The ratio of Ni/ Nf increases with the increase of strain amplitude. As the cyclic stress-strain curves shown in Fig.4, at high strain amplitudes, the specimens fail rapidly and the stress amplitudes could not decreased sufficiently before failure The gradual decreasing trend was apparent at low strain amplitudes due to the slow crack propagation speed. In contrast, the defects in the weld joint may be attributed to earlier crack initiation and scattered fatigue data.

Fig. 10 shows the percent of fatigue crack initiation life to total life Ni/ Nf at different strain amplitudes. For the base metal, by fitting the test data using the least-square method, the strain-fatigue crack initiation life relationship can be obtained as:

$$N_f^{'} = 5 \times 10^{-4} \left(\varepsilon_a \right)^{-2.818} \qquad (6)$$

where ε_a is the uniaxial strain amplitude, and N_f is the crack initiation life. In addition, we can see from Fig.10 that the fitting curve of welded joint does not agree well with the test data. Hence, the prediction method is not applicable for the welded joint.

2.4 Energy-life relationship

In addition to strain-life and stress-life relationships, a further means to predict fatigue failure is by consideration of energy dissipation [5, 21]. A closed curve can be plotted by tracing stress-strain at each cycle during fatigue test, known as hysteresis loop. The area of the loop represents the dissipated energy

during this cycle. Therefore, the total area of all hysteresis loops can represent the dissipated energy during the whole life which describes the ability of the material to resist cyclic plastic deformation.

The hysteresis loop at the stabilized cycle can be used to calculate the plastic strain energy density range according to the following expression:

$$\Delta W_P = 2\int_0^{\Delta\varepsilon} \Delta\sigma d(\Delta\varepsilon) - \Delta\sigma\Delta\varepsilon \tag{7}$$

From the test results, it is found that the base metal and welded joint both exhibit Masing cyclic stress-strain behavior. Thus, the plastic strain energy can be given as the function of cyclic hardening exponent 'n', cyclic stress amplitude $\Delta\sigma$ and plastic strain amplitude $\Delta\varepsilon_p$ as follows [22]:

$$\Delta W_P = \frac{(1-n')}{1+n'}\Delta\sigma\Delta\varepsilon_P \tag{8}$$

The calculation results and experimental data of both the base metal and welded joint are plotted in Fig.12. It can be seen that the data is conservative and that the parameters obtained from the cyclic stress-strain relationship are well applicable to this model with the error less than 25%. Notably, in the calculation, the adopted plastic energy and parameters in cyclic stress-strain relationship are based on the hysteresis loop at half number of cycles to failure rather than all the hysteresis loops during the whole life [7,20], and this approximation may lead to the calculation error mentioned above.

Substituting Eqs. (2),(4) and (5) into Eq.(8), the relationship between plastic energy and fatigue life can be obtained as:

$$\Delta W_P = 4\sigma_f'\varepsilon_f' \frac{(1-n')}{1+n'}(2N_f)^{b+c} \tag{9}$$

where the terms are defined as aforementioned. This equation can be used to predict fatigue life of the Q345 base metal and its welded joint for lack of experimental data.

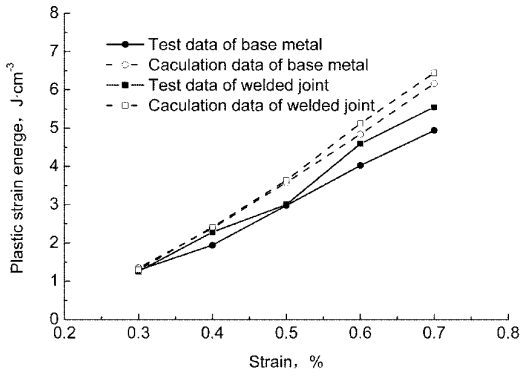

Fig.12 Relationship between strain amplitude and plastic strain energy

3 Conclusions

Low cycle fatigue tests of Q345B base material and its welded joint were carried out in this study. The test results revealed that:

1) Q345B showed significant cyclic hardening when the strain amplitudes are larger and cyclic softening when the strain amplitudes are lower than 0.4%. The weld joints showed cyclic hardening in the whole strain regime of 0.3%~0.7%.
2) Welded joint showed lower fatigue strength than the base metal. The low cycle transition life of the welded joint decreased by 60% than the base metal. The fatigue strength of the weld joints at 2000 cycles was found 79% of that of the base metal. The fatigue life of the weld joints was 85% of that of

the base metal at the strain amplitude of 0.7%, and was only 52% at the strain amplitude of 0.3%. It was concluded that mechanical inhomogeneity of the weld joints decreased the low cycle fatigue properties of the smooth welded joint.

3) Material parameters for strain-life relationships and cyclic stress-strain curves of the base metal and welded joint were obtained from the test results.
4) Fatigue life predictions for the base metal and welded joint were developed from energy dissipation theory.

Acknowledgments

The authors gratefully acknowledged the financial supports from the National Science Foundation of China (NSFC- 11172188, 11302142) and the International Collaboration Project of Ministry of Science and Technology (2012DFG51540) .

References

[1] V.Subramanya Sarma, K.A.Padmanabhan. Low cycle fatigue behaviour of a medium carbon microalloyed steel, Int J. Fatigue, 29(1997):135-140.
[2] E.S. Puchi-Cabrera,R.A. Saya-Gamboa, J.G. La Barbera-Sosa, et. Fatigue life of AISI 316L stainless steel welded joints, obtained by GMAW [J]. Welding International, 2009, 23(10):778-788.
[3] Y.R. Luo, C.X. Huang, R.H. Tian, Q.Y. Wang. Effects of strain rate on low cycle fatigue behavior of high-strengh structural steel. J Iron Steel Res Int, 20(2013):50-56.
[4] Yan X. Low cycle fatigue and cyclic stress ratcheting failure behavior of carbon steel 45 under uniaxial cyclic loading. International Journal of Fatigue, 2005, 27(9):1124-32.
[5] Rozumek D., Marciniak Z.. Fatigue properties of notched specimens made of FeP04 steel. Materials Science, 2012, 47(4): 462-469.
[6] K.H. Nip, L. Gardner , C.M. Davies, A.Y. Elghazouli. Extremely low cycle fatigue tests on structural carbon steel and stainless steel. Journal of Constructional Steel Research, 2010,66,96-110.
[7] Bergengren Y, Larsson M, Melander A. Fatigue properties of stainless sheet steels in air at room temperature. Materials Science and Technology 1995;11(12):1275-80.
[8] Kanazawa K, Miller K J, Brown M W. Low cycle fatigue under out-of-phase loading conditions. Journal of Engineering Materials and Technology, 1977, 99：222-228.
[9] Callaghan M D, Humphries S R, Law M, et al. Energy-based approach for the evaluation of low cycle fatigue behaviour of 2.25Cr--lMo steel at elevated temperature. Materials Science and Engineering, 2010, 527 (21/22): 5619-5623.
[10] Ellyin F, Asada Y. Time-dependent fatigue failure: the creep fatigue interaction. International Journal of Fatigue,1991, 13(2): 157-164.
[11] Fricke W . Fatigue analysis of welded joints:state of development. Marine Structures, 2003， 16, 185–200.
[12] Puchi-Cabrera E.S., Saya-Gamboa R.A., La Barbera-Sosa J.G., et al. Fatigue Life of AISI 316L Stainless Steel Welded Joints, Obtained by GMAW. Welding International, 2009, 23, 778-788.
[13] Teng T.L., Chang P.H. Effect of residual stresses on fatigue crack initiation life for butt-welded joints. Journal of Materials Processing Technology, 2004,145, 325–335.
[14] Standardization Administration of the People's Republic of China. GB/T 15248-1994, The Test Method for Axial Loading Constant-Amplitude Low-Cycle Fatigue of Metallic Materials. Beijing: China Standards Institution, 1994.
[15] K.H. Nip, L. Gardner , C.M. Davies, A.Y. Elghazouli. Extremely low cycle fatigue tests on structural carbon steel and stainless steel[J]. Journal of Constructional Steel Research, 2010, 66, 96-110.
[16] Troshchenko V.T. and Khamaza L.A.. Investigation of deformation diagrams of metals under static and cyclic loads in relation to their fatigue failure. Strength of Materials, 1976, 8(9):1052-1056.
[17] Coffin Jr LF. A study of the effects of cyclic thermal stresses on a ductile metal. Transactions of ASME 1954;76:931-50.
[18] Manson SS. Behaviour of materials under conditions of thermal stress. National Advisory Commission on Aeronautics: Report 1170. Cleveland: Lewis Flight Propulsion Laboratory; 1954.
[19] M.M. Alam , Z. Barsoum , P. Jonsén, A.F.H. Kaplan, H.Å. Häggblad. Influence of defects on fatigue crack propagation in laser hybrid welded eccentric fillet joint, Engineering Fracture Mechanics, 2011,78:2246-2258
[20] Chen Long, Cai Li-xun. The low cycle fatigue crack growth prediction model based on material's low cyclic fatigue

properties [J]. Engineering Mechanics, 2012,29(10):34-39.

[21] Morrow J. Cyclic plastic strain energy and fatigue of metals. Internal fraction, damping and cyclic plasticity. ASTM STP 378,1965:48-84.

[22] Callaghan M D，Humphries S R，Law M，et al. Energy based approach for the evaluation of low cycle fatigue behavior of 2.25Cr-1Mo steel at elevated temperature. Journal of Materials Science and Engineering: A, 2010,527(21/22) :5619-5623.